Adlayers of Keggin Type Polytungstate Anions on Platinum: Negligible Electrochemical Signatures and Manifestations of "Molecular UPD"

Elena D. Mishina,[†,§] Galina A. Tsirlina,*[,‡] Elena V. Timofeeva,[‡] Nataliya E. Sherstyuk,[†] Marina I. Borzenko,[‡] Nobuko Tanimura,[§] Seiichiro Nakabayashi,[§] and Oleg A. Petrii[‡]

Moscow Institute of Radioengineering, Electronics and Automation, prosp. Vernadskogo, 78, 117454 Moscow, Russia, Department of Electrochemistry, Moscow State University, Leninskie Gory 1-str.3, 119992 Moscow, Russia, and Department of Chemistry, Faculty of Science, Saitama University, Saitama 338-8570, Japan

Received: June 11, 2004; In Final Form: August 27, 2004

Second-harmonic generation and electrochemical techniques are applied to characterize the adsorption of Keggin type heteropolyanions (P- and Si-dodecatungstates) on polycrystalline platinum. Optical signal confirms polytungstates adsorption in the overall potential range (0.04−1.3 V vs RHE) even for low concentrations, when adsorption manifestations in cyclic voltammograms are negligible. Basically, the dependence of adsorption on electrode potential is typical for inorganic anions (increase of coverage with potential in the hydrogen and double-layer regions and weakening of adsorption in the oxygen region). An unusual interaction with hydrogen adatoms H_{ad} is discovered, and similarity with spillover-like phenomenon is mentioned. The adsorbate−platinum interactions depend on both potential and nature of adsorbed species. These observations are qualitatively interpreted in terms of partial charge transfer from Pt to tungstate which is equivalent to partial W(VI/V) reduction at potentials more positive than the equilibrium potentials of the corresponding W(VI/V) redox pairs in solution bulk (molecular UPD). A qualitative model is proposed for polytungstate interaction with adsorbed oxygen, which explains the observed hysteresis phenomena.

Introduction

Highly symmetric Keggin polyoxometalate anions present the intriguing and attractive components of a toolbox for nanotechnology.[1−3] These compounds are also recognized as the multifunctional catalysts and electrocatalysts[4−6] and materials for electrochromic and photochromic devices.[7] The majority of these applications are closely related to the problem of immobilization at the solid surfaces, in which context both the monolayer adsorption of oxometalates and multilayer film formation are of crucial importance.

Strong chemosorption of various oxometalates, including most easily available Keggin anions on metallic and carbon electrodes, was discovered during the past decade.[8−21] Several physical techniques confirmed the formation of self-assembled monolayers (however, this process is rather slow in some systems). The most advanced molecular level results were obtained for Ag,[10−12,14,15] which demonstrate strong covalent interaction with Keggin anions. A similar type of adsorption was found for the positively charged mercury.[8,20,21] The dependence of polytungstate adsorption on electrode potential (charge) was also reported for carbon.[13] The adsorption on gold is doubtless[9,16] or at least less strong.[11,12,15] As it follows from systematic ex-situ tunneling spectroscopic studies (see refs 18 and 19 for example), the electronic properties of surfaces modified with adsorbed heteropolyanions correlate with corresponding W(VI/V) redox potentials.

Surprisingly, the interaction of heteropolyanions on Pt attracted lower attention, despite the evident indirect manifestations of pronounced adsorption.[22,23] Data presented below for phosphododecatungstate and silicadodecatungstate (denoted as PW12 and SiW12, respectively) demonstrate that adsorption takes place in a wide potential range, and its specific features (as compared with adsorption at other metals) result from the interaction with hydrogen adatoms. The latter appears to be an additional important factor inducing the interplay with free electrode charge effects.

Experimental Section

Reactants. $H_3PW_{12}O_{40}*nH_2O$ and $H_4SiW_{12}O_{40}*nH_2O$ (Merck) were first characterized by UV−vis spectra measurements in 0.5 M H_2SO_4 solution. Absorption was proportional to concentration in the overall available range (5−50 μM). To waive an uncertainty of n value, two substances with known water content were used for comparison: $H_3PW_{12}O_{40}*30\ H_2O$ (synthesized according to ref 24) and $H_3PW_{12}O_{40}*7H_2O$ (provided by Reactive Co., Russia). It was concluded that for Merck heteropoly acids $n = 7$. The molar extinction coefficient at 265 nm equals 37000 $M^{-1}\ cm^{-1}$. This value is slightly lower than that reported in ref 25, and the difference can be explained by different ratios of α- and β-isomers.[26] To check possible effects of impurities, both abovementioned substances and sodium salt $Na_3PW_{12}O_{40}*nH_2O$ (Fluka) were used for comparative electrochemical experiments. No difference of any voltammetric features was observed. Sulfuric acid of analysis grade quality (Merck or Wako) and Milli-Q water were used for solution preparation. For electrochemical fabrication of solid oxotungstate film, deposition solution was prepared with the use of $Na_2WO_4*2H_2O$ (Merck).

Electrochemistry. Cyclic voltammograms and current transients were measured in a three-electrode cell with separated

* Author to whom correspondence should be addressed.
[†] Moscow Institute of Radioengineering.
[‡] Moscow State University.
[§] Saitama University.

10.1021/jp047470q CCC: $27.50
Published on Web 10/08/2004

compartments equipped for high-quality deaeration (Ar). The electrode consisted of polycrystalline Pt foil (geometric surface area 1−2 cm^2) attached to Pt wire soldered up in glass holder. In several experiments, this electrode was platinized from 1 wt % H_2PtCl_6 solution (high-purity grade $H_2PtCl_6 \cdot H_2O$, Reakhim, Russia) at constant potential mode (0.25 V RHE). Platinization time was varied to obtain various roughness factors. Reversible hydrogen reference electrode (RHE) was used which consisted of platinized platinum (Pt/Pt) plate in supporting electrolyte solution saturated with H_2 (1 atm). All data for platinum are reported with the use of RHE scale.

DC polarography (DME, mercury flow rate 6.5 mg/s, open circuit drop life 10.1 s, deaeration with H_2) was performed in nonseparated cell with Pt foil anode and reference saturated calomel electrode (SCE). To make easier the comparison with literature data, we keep this potential scale for polarograms presentation. As solution pH was 0.45 ± 0.01, E(RHE) = E(SCE) − 0.267 V for all solutions under study. Currents were recorded at the end of the drop lifetime.

In both CV and polarographic cells, Luggin capillary was inserted to minimize ohmic contribution.

For optical measurements, nonseparated electrochemical glass cell was used with quartz bottom optical window. Working electrode surface was presented by the face of Pt rod inserted in PTFE holder. This mechanically polished surface was located parallel to the bottom (window). Coiled Pt wire of large surface area (counter electrode) was located at the periphery of the cell. Reference electrode (SCE) was separated with a glass cock (no Luggin capillary). Ar was bubbled steadily during the measurements. The quality of deaeration in optical experiments was lower than in more perfect electrochemical cells. However, all CV recorded in parallel with optical measurements were very close to CV obtained as described above.

The same cell was applied for electrodeposition of oxotungstate film according to the original technique proposed in ref 27. Briefly, Na_2WO_4 was dissolved in boiling water, and then concentrated sulfuric acid was added. This technique allowed to obtain long-lived metastable acidic tungstate solution 0.5 M H_2SO_4 + 1 mM Na_2WO_4. During potential cycling in this solution (0.05−1.1 V (RHE), 50 mV/s), a film of nonstoichiometric hydrated tungsten oxide (tungsten bronze) was built up at the surface of the Pt electrode.

To obtain a standard clean electrode surface, platinum foil was etched in aqua regia, thoroughly washed, and subjected to subsequent anodic and cathodic polarization in supporting electrolyte solution. When etching was impossible (Pt/Pt or Pt in PTFE), cleaning was restricted to the latter electrochemical treatment. The purity of surface was always confirmed by the quality of H−UPD region (CV in supporting electrolyte).

Pt true surface area and roughness factor were estimated from hydrogen desorption charge (assumed to be 0.21 mC/cm^2 after double-layer correction). All current and charge densities are reported below per true surface area.

Potentiostates used in the experiments were PARC273 equipped with PR-8 generator and Potentiostate/Galvanostate 2020 Toho Technical Res. with function generator HB111, Hokuto Denko.

In-Situ Second-Harmonic Generation (SHG). A fundamental radiation of a Ti:Sapphire laser was used at wavelength 760 nm with a pulse width of about 100 fs and repetition rate of 78 MHz. Laser radiation of 400 mW was focused onto a circular spot of ca. 0.25-mm size. This gives the pulse energy density of 8 $\mu J/cm^2$, far beyond the energy of photoinduced processes on the Pt surface.[28−31] However, the necessary checks of noninvasive character of the laser radiation influence on the studied system was performed: the power law for the second-harmonic radiation $I^{2\omega} \propto (W^{\omega})^n$ (up to 800 mW of average power it gave $n = 2$), and also reversibility of SHG intensity and current in repetitive voltage cycles, with cyclic voltammograms being coincident with and without laser irradiation application.

The incident angle of fundamental radiation was 35° and all cell configurations were kept constant in each experimental series; the changes of solution composition were achieved by adding drops of concentrated solutions from the top of the cell.

SHG generation at 380 nm was discriminated specroscopically by appropriate color and band-pass filters. A photon-counting system was used for detection. The background did not exceed several phot/s. For in-situ optical measurement, the signal from potentiostate was processed by analog-to-digital converter NI5911 through the BNC2110 connector (National Instr.).

The SHG signal was accumulated over 1 s for each point. The total measuring time was up to 2500 s (which usually corresponded to 8−10 complete CV scans). The resulting set of points was later averaged over the number of scans for each potential.

Results and Discussion

Cyclic Voltammetry: Contribution of Mass Transport Controlled Redox Process. It is not so easy to apply the traditional approach to the studies of adsorption on Pt (on the basis of the effects of adsorbate on H− and O−UPD) to Keggin anions under consideration. The reason is a superposition of redox processes taking place in the H−UPD region. This is easy to see from Figure 1, especially for high (10 mM) SiW12 (a) and PW12 (b) concentrations. Stirring of solution with Ar bubbles affected only anodic branch of the curves in the H−UPD region (insert in Figure 1). The decrease of anodic current in this region was more pronounced for slower scan rates and higher concentrations. This means that the species undergoing oxidation are not surface-attached but are located in the diffusion layer.

The mixed nature of currents (adsorption + reversible redox reaction) is confirmed by concentration dependence of currents. Additionally, no exact linearity is found either for current j versus scan rate υ plot or j versus $\upsilon^{1/2}$ plot. It was easy to expect for PW12 which redox potential is significantly positive in RHE scale.[32] As for SiW12, the result looks less foreseeable because the values of polarographic half-wave potentials[33] and voltammetric formal potentials[34,35] depend on the electrode and supporting electrolyte nature.

To avoid any contradictions, we applied DC polarography (DME) to solutions under study (left-hand part in Figure 2). For DME, much more negative values of potential are achievable because of negligibly slow hydrogen evolution. The behavior of polarographic waves (especially of the first wave) appeared to be much more complex than mentioned in refs 32 and 33, in particular because of polarographic maxima. Complications are more pronounced for higher Keggin anion concentration.

The polarographic half wave potentials $E_{1/2}$ for the first reduction wave of PW12 were −0.17 ÷ −0.13 V (SCE), shifting toward more negative direction with PW12 concentration in the 0.5−2 mM range. The same tendency was observed for SiW12 (concentration-dependent $E_{1/2}$ = −0.34 ÷ −0.28 V (SCE), more negative for higher concentrations). The accuracy of diffusion coefficient calculation was rather low because of very short and

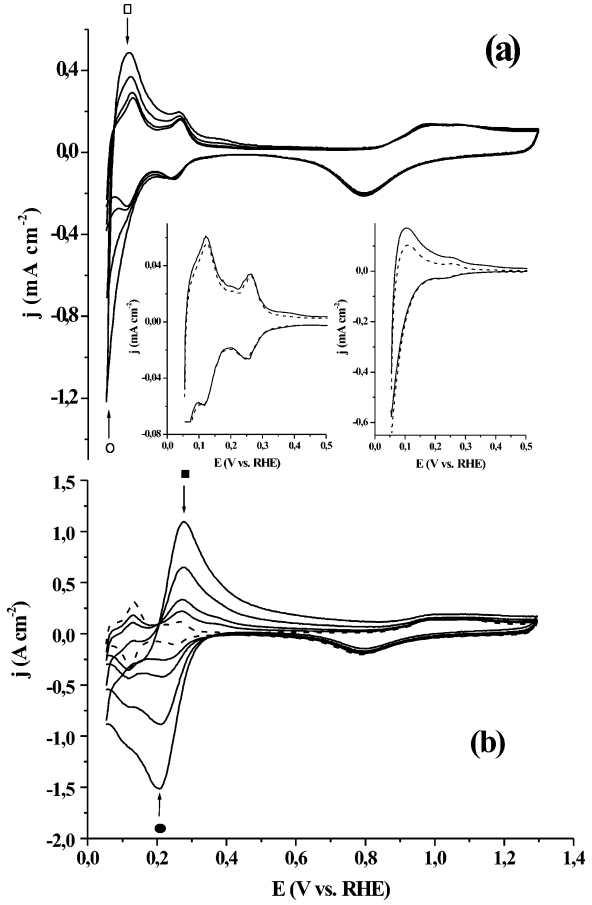

Figure 1. Cyclic voltammograms measured in 0.5 M H_2SO_4 solution with SiW12 (a) and PW12 (b) additives. Dashed curves correspond to supporting electrolyte, for other curves the subsequent increase of current corresponds to increase of reactant concentration (1, 2, 5, 10 mM). Insert presents the effect of solution stirring with Ar bubbles (dotted curves) for 1 (left) and 10 (right) mM SiW12 at scan rate 20 mV s^{-1}.

sloping plateaus between the two first waves. All the values fall into the interval of $(2.5-4.5)*10^{-6}$ cm^2 s^{-1}, in satisfactory agreement with ref 32.

To compare $E_{1/2}$ and formal potentials observed for Pt electrode, we subtracted CV for Pt in supporting electrolyte solution from CVs measured in the presence of Keggin anions. Such subtracted CVs are given at the right-hand part (Figure 2) for 10 mM PW12 (solid curve) and SiW12 (dashed curve). It is easy to see that formal potential of PW12 is shifted toward more positive values as compared with polarographic $E_{1/2}$. At the same time, the formal potential estimated by these means is only 20−25 mV more positive than the value reported in ref 32 (arrow). It is difficult to do similar comparison for SiW12, for which only a portion of subtracted CV on Pt is available at positive RHE potentials, but the tendency looks very similar.

We can conclude that the redox behavior of Keggin anions in sulfuric acid on Pt is reversible (or at least more reversible than on mercury), indicating qualitative difference in adsorption of polyoxotungstates on Hg and Pt. As additional illustration of the interplay of diffusion-controlled redox processes and adsorption contributions, we present CVs for a set of platinum electrodes of various roughnesses (Figure 3). The evolution of CV shape in H−UPD region at fixed PW12 concentration is similar to the concentration-induced evolution for smooth Pt (Figure 1). Redox process predominates when the roughness is low but becomes virtually insignificant at high roughnesses. This means that redox transformations of PW12 take place only on

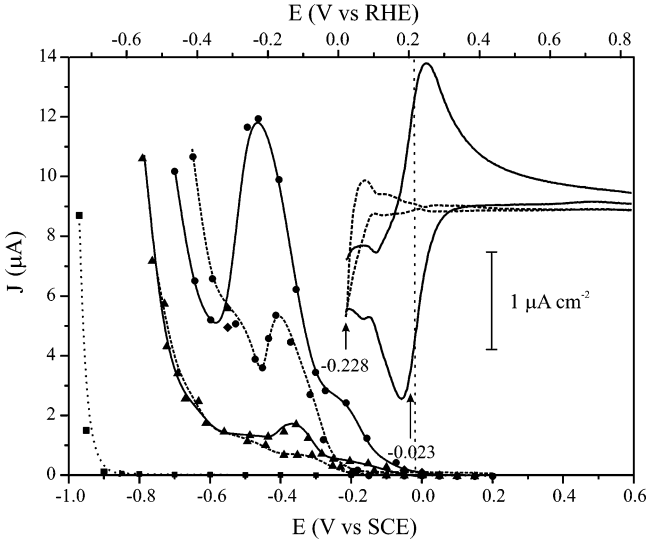

Figure 2. Comparison of polarographic data (Hg, points, left-hand side) and subtracted cyclic voltammograms (Pt, right-hand side) for reduction of PW12 (solid lines) and SiW12 (dashed lines) in 0.5 M H_2SO_4. Polarogram of the supporting electrolyte (dotted) is given for comparison. Reactant concentrations: 10 mM for voltammograms and 2 mM (circles) and 0.5 mM (tirangles) for polarograms. Both SCE and RHE potential scales are presented to simplify the comparison with literature data. Arrows correspond to $E_{1/2}$ values from ref 32 (SCE scale).

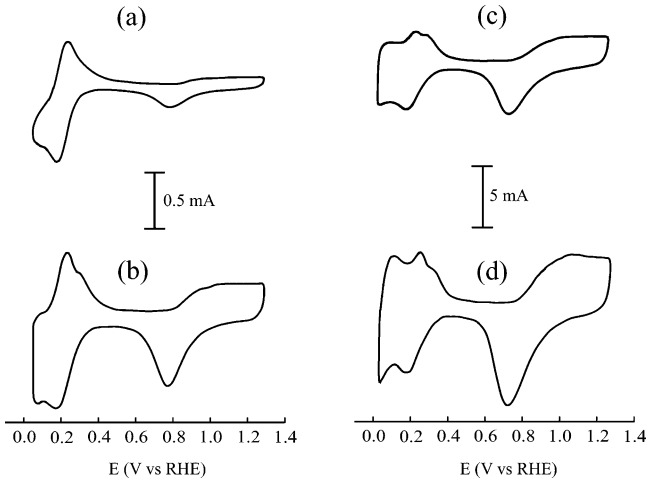

Figure 3. Cyclic voltammograms in 0.5 M H_2SO_4 + 10 mM PW12 solution measured on Pt/Pt electrodes of various roughness factors: 11 (a), 40 (b), 270 (c), and 545 (d). Scan rate 10 mV s^{-1}.

external surface of Pt/Pt, which contribution decreases with roughness. This result confirms again the predominating mass transport control for the observed reaction.

The shape of subtracted CV for SiW12 (Figure 2, dashed curve) is rather complex. This curve consists of a truncated pair of peaks and an additional feature starting at $E > 0.1$ V (RHE). The same excess charge is obtained for PW12 if the concentration of reactant is lower and the accuracy of background subtraction is satisfactory. The adsorption nature of this unusual feature is discussed below.

Direct and Indirect Manifestations of Polytungstate Adsorption. The studies of adsorption of inorganic anions on Pt metals form one of the milestones of a famous thermodynamic theory,[36] which ties together the ionic adsorption and UPD phenomena. It is typical for strongly adsorbing anions (for example, halides) to suppress H− and O−UPD partly but simultaneously to add their own contribution into the total

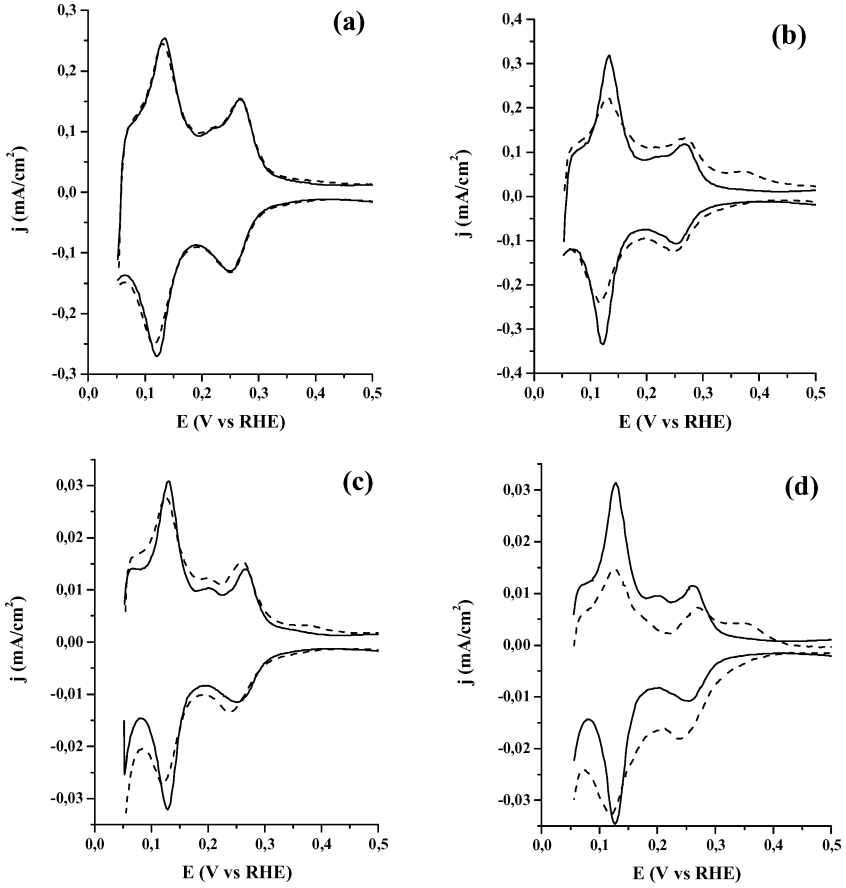

Figure 4. Representative cyclic voltammograms corrected for contribution of redox process measured in 0.5 M H_2SO_4 + 1 mM SiW12 (a,c) and 0.5 M H_2SO_4 + 1 mM PW12 (b, d) (solid curves correspond to background); scan rates 100 (a, b) and 10 (c, d) mV s^{-1}.

surface charge. Mutual effects of anions and adatoms[37] result in redistribution of charge along potential axis, with the shift of the H−UPD region toward more negative potentials, when the O−UPD region moves toward more positive potentials. The polarization capacity in the double-layer region tends to decrease in halide solutions as compared to media containing less adsorbing anions.

The effects induced by polytungstate adsorption do not agree with these tendencies and are barely perceptible, especially at high scan rates. Typical situations are presented in Figure 4 constructed by using the inverse procedure as compared to CVs in Figure 2; redox contributions are subtracted. To provide a higher accuracy of these procedures, we used CV for 20 mM solution for which in the H−UPD region the ratio of redox and adsorption contributions is ca. 100:1. The redox contribution is proportional to bulk concentration, so we subtracted concentration-normalized CV of more concentrated solution from CV of more dilute solution. Certainly, it makes sense only when the difference in concentrations is pronounced. [Some inaccuracy appears because a low fraction of adsorption contribution is also subtracted (1/20 for concentrations discussed above). This leads to a small underestimation of the resulting currents in diluted solution but falls into usual limits of coulometric inaccuracy (few percents).] For data in Figure 4, this difference exceeds 1 order of magnitude.

The effects for which this subtraction procedure gives reliable results are as follows.

(1) Total charge in the H−UPD region increases slightly; total effect results from the decrease of current in the region of weakly adsorbed hydrogen (E < 0.15 V) and its increase at higher potentials (Figure 4b−d). All effects are more pronounced at lower scan rate (dashed curves). The total H−UPD charge equals background charge plus excess charge; the latter amounts to no more than 10−25% of the usual charge spent for formation of hydrogen monolayer (Figure 4). Reliability of higher values (ca. 50% for 10 mM PW12) is doubtful because the subtracted value heavily exceeds the resulting purpose value.

(2) "H−UPD" region spreads and occupies more wide area than in supporting electrolyte solution (most pronounced in Figure 4b,d), up to E = 0.45 V (this part is included into charge balance in Figure 5b).

(3) Charge in the double-layer region increases slightly.

(4) Decrease of charge in the O−UPD region (0.7 < E < 1.3 V) takes place, which reliably the accuracy of coulometric estimates only for high PW12 concentrations (Figure 5b). Suppression of O−UPD at E < 1.0 V is partly compensated by additional oxygen adsorption at E > 1.0 V, both effects being only slightly dependent on scan rate.

Effects 2−4 present no complications because they can be observed directly without subtraction. However, for the majority of solutions under study (especially for SiW12), they look negligible. Effect 1, which requires the subtraction procedure, is on the verge of coulometric accuracy for low concentrations. The higher accuracy of the excess charge estimates can be achieved for Pt/Pt, especially for high roughness (like in Figure 3b−d) with a very low ratio of diffusion-controlled and adsorption contributions. The resulting values for 10 mM PW12 amount to 25, 25, and 15% of background H−UPD charge for roughness factors 40, 270, and 545, respectively. The lower value for the highest roughness under study can result from a more complex shape of Pt/Pt pores and rise of steric limitations for large anions to penetrate. Estimates for Pt/Pt confirm that

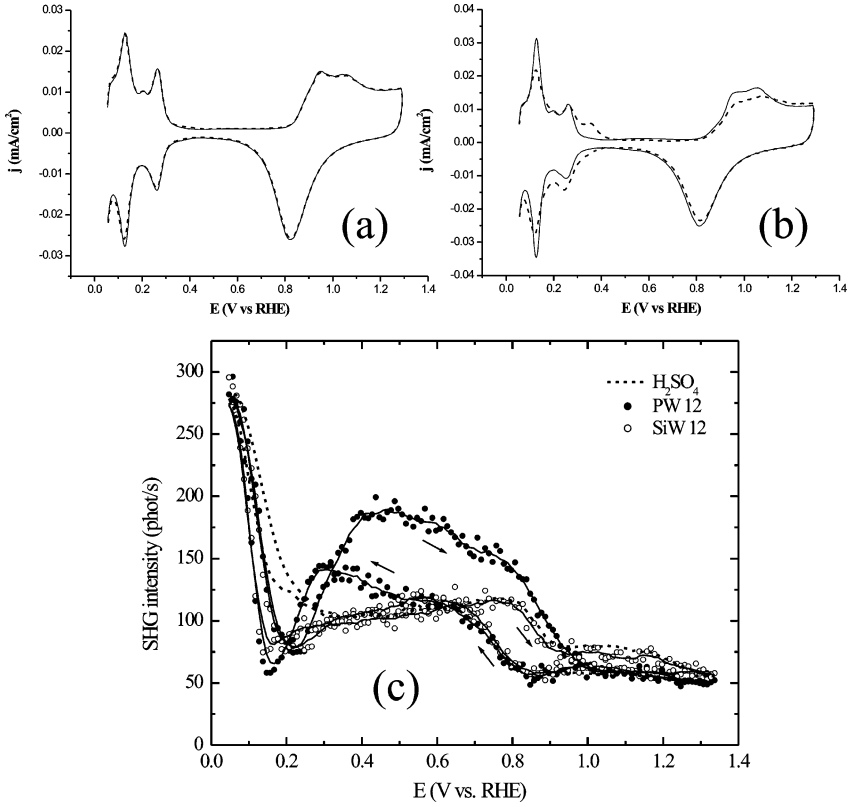

Figure 5. Cyclic voltammograms corrected for contribution of redox process measured in 0.5 H_2SO_4 (solid curve) and in the same solution containing 0.5 mM SiW12 (a) and 0.5 mM PW12 (b) (dashed curves); (c) SHG vs potential dependences measured in 0.5 H_2SO_4 (dotted curve) and in the same solution containing 0.5 mM PW12 (solid symbols) and 0.5 mM SiW12 (open symbols). Scan rate 10 mV s^{-1}.

the values of excess charge for Keggin anions on platinum are significant.

However, glancing at data for smooth Pt with minor effects at low concentrations, especially Figure 4a, one can ask: "Probably they do not adsorb at all?". The answer immediately appears in Figure 5. It comes from SHG data for 0.5 mM solutions of polytungstates. For SiW12, this concentration is too low to observe any effects in CV (Figure 5a); for PW12, the excess charges are rather small (<10%) but already noticeable (Figure 5b). However, SHG (Figure 5c) turns out to be more sensitive and unmasks the adsorbed polytungstate species. This situation is rather unusual because Pt is a metal with very low SHG response[38−46] as compared, to say, to Au and Ag. For all currently studied adsorbates, electrochemical techniques are able to discover much finer features of Pt/solution interface than SHG. For polytungstates, we observe for the first time an opposite situation.

The following effects are observed at SHG versus potential dependences.

(1) Decrease of SHG signal in the region of so-called weakly bonded hydrogen < 0.20−0.25 V RHE.

(2) Increase of the SHG signal in the double-layer region (for PW12); it is also observed for SiW12 at higher concentrations, Figure 6a.

(3) Pronounced hysteresis of the SHG curve in the double-layer region, which is completely absent from the background dependence (dashed curve in sulfuric acid solution).

(4) Small decrease of the SHG signal in the O−UPD region corresponding to mid oxygen coverages accompanied by almost complete disappearance of SHG hysteresis.

Possible Reasons of SHG Increase and Decrease. Within the simplest approach, the nonlinear optical response of metal electrode in electrochemical environment can be described by nonlinear polarization of a metal $P^m(2\omega)$ and adsorbate $P^{ad}(2\omega)$: $P(2\omega) = P^m(2\omega) + P^{ad}(2\omega)$.

Generally, $P^m(2\omega)$ is anisotropic, that is, depends on the crystallographic orientation of the surface. For polycrystalline electrode, only isotropic component survives, $P_{iso}{}^m(2\omega)$, and anisotropic contribution averages to zero over randomly oriented microcrystallites. According to ref 47, isotropic nonlinear polarization of the metal is modified by a total charge transfer σ from a metal to adsorbate and in the frame of a jellium model can be written as

$$P_{iso}{}^m(2\omega) \propto a_0 + \Delta a(\sigma)$$

where Rudnick−Stern parameter $a_0 < 0$.

Nonlinear polarization of adsorbate $P^{ad}(2\omega)$ can be described as

$$P_i{}^{AD}(2\omega) = \gamma^{ad}\theta E_j(\omega)E_k(\omega)$$

where γ^{ad} and θ are the first hyperpolarizability of adsorbate and surface coverage, respectively.

Thus, adsorption of ions and molecules on the metal surface may change the total SHG signal by the following:

(1) Modification of the metal SHG response owing to (i) change of surface coverage with constant charge transfer, (ii) change of a charge transfer of individual species (zero-order polarizability) with constant coverage, and (iii) simultaneous change of surface coverage and zero-order polarizability.

(2) Direct SHG response form adsorbate, which is proportional for surface coverage.

The presented model is quite qualitative. So, we escape any quantitative considerations at this stage. To interpret SHG data, we need first to discuss briefly the nature of the background

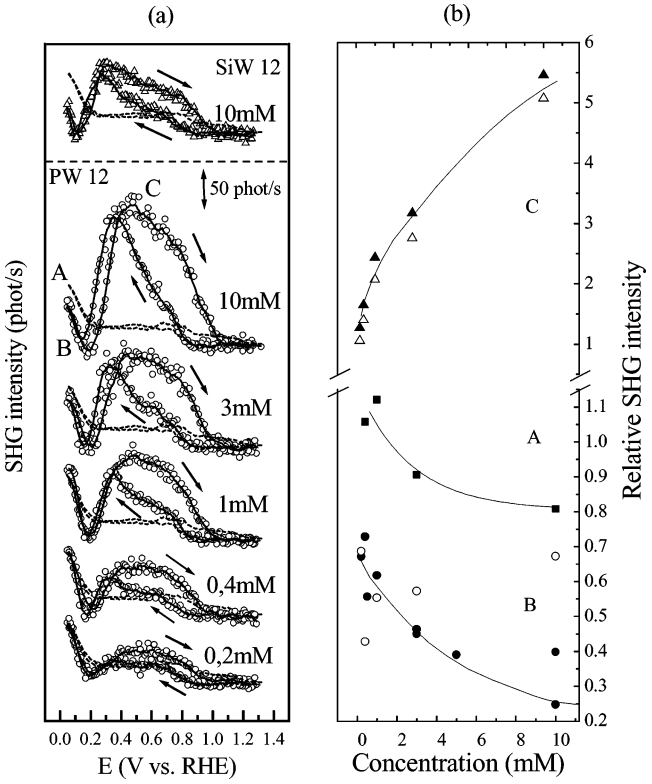

Figure 6. Concentration dependence of SHG vs potential curves for 0.5 H_2SO_4 + PW12 and 0.5 H_2SO_4 + 10 mM SiW12 (top) (a) and the relative SHG intensities at certain characteristic points (b). A (solid squares), 0.04 V (RHE); B (circles), at minima; C (triangles), at maxima. For B and C, solid points correspond to anodic and open to cathodic scans. Scan rate 10 mV s^{-1}. Data for SiW (gray points, anodic scans) are given for comparison.

signal for each potential region. Unfortunately, SHG was only occasionally studied on polycrystalline platinum because of relatively low signals, and all interpretations proposed earlier are rather simplified. More detailed analysis of SHG signal is beyond the frame of this paper and will be presented in a separate communication. Now we concentrate on the qualitative effects and search for similarities/contrasts in SHG behavior of polytungstates and other adsorbates.

SHG in H−UPD Region. The increase of SHG in the region of "weakly bonded hydrogen" (high hydrogen coverages) was observed for polycrystalline platinum in various solutions, frequencies, and incident angles.[38−43] It also appears in SHG of microfacetted Pt(111)[44] and platinum single crystals,[45,46] which data are not used below for comparison because of pronounced anisotropic contribution to $P^{m}(2\omega)$ absent in our work. Low sensitivity of hydrogen response to frequency value and surface geometry (as follows from ref 39, the effect is more sensitive to light polarization) makes it possible to consider its nature in the framework of rather simplified statements discussed, for example, in ref 43 (dominating $P_{iso}^{m}(2\omega)$ contribution, which demonstrates adsorbate-induced increase of electron surface density). Correspondingly, under the first approximation two factors can be considered as responsible for SHG growth, namely, degree of charge transfer (from H adatom to metal) and surface coverage. The increase of SHG response with hydrogen coverage is not unique for electrified platinum/solution interface, and it was also reported for gas-phase adsorption.[48] So, we believe that specific state of hydrogen coadsorbed with water can hardly be a reason of this effect.

The concept of Pt−H effective dipole was discussed long ago in the framework of thermodynamic analysis.[49] Despite the

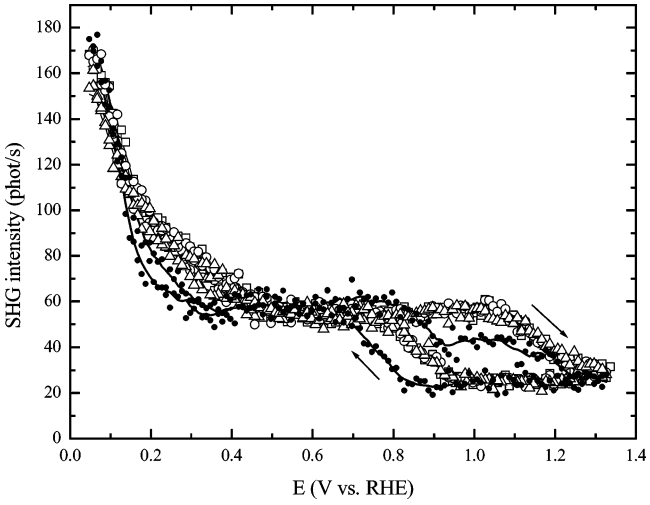

Figure 7. SHG vs potential curves for 0.5 H_2SO_4 + HCl series. Solid circles, 0.5 H_2SO_4; open symbols correspond to 2 (squares), 4 (circles), and 10 (triangles) mM HCl additive. Scan rate 10 mV s^{-1}.

uncertainty of attribution of transferred charge to metallic or solution part (which is unavoidable in such analysis),[50,51] the assumed change of the effective dipole orientation corresponds to the potential dependent degree and sign of charge transfer at Pt/(H_2O, H_{ad}) interface. This change accompanies the increase of free surface charge. The potentials of zero free charge (pzfc) for Pt/0.5 H_2SO_4 solution were never determined with the use of a purely thermodynamic approach,[36] which provides high accuracy. However, from pH- and concentration dependences of pzfc obtained from titration under constant charge mode,[52−54] this potential value can be extrapolated, with resulting value of 0.25 ± 0.02 V. It is very close to the value at which the hydrogen-induced SHG increase starts (dashed curve in Figure 5c).

The decrease of SHG signal in the left part of H−UPD region takes place in the presence of Keggin anions (Figure 5c). This effect becomes more and more pronounced with concentration (Figure 6a, bottom curve in Figure 6b). Taking into account the abovementioned nature of SHG, one can assume one of the following versions:

(1) Hydrogen coverage is decreased in the presence of polytungstates, and no compensating contribution goes from adsorbed anions.

(2) The degree of charge transfer from H adatoms to Pt decreases (and even changes its sign), when the coverage changes slightly or remains constant.

Our starting point for future choice of realistic hypothesis is the comparison of the discussed SHG dependences with SHG behavior in the presence of more studied inorganic anions. The effect observed for HCl additives under the same experimental mode (Figure 7) is totally opposite: for $0.2 < E < 0.4$ V, SHG signal increases independently on chloride concentration. Additionally, the SHG rise starts at more positive potentials (boundary value ca. 0.40−0.45 V (RHE)). An opposite pzfc shift to more negative potentials is induced by chloride.[33] This means that SHG signal at $E < 0.45$ V cannot be uniquely referred to hydrogen adatoms, and one should assume nonzero $P^{Cl}(2\omega)$.

SHG behavior in halide-containing solutions was reported earlier in refs 39 and 43. Direct comparison is complicated because of perchloric supporting electrolyte and different modes of optical measurements, but qualitatively the effects are similar. Chloride contribution to SHG is pronounced just in the region of potentials for which the potential-dependent degree of charge

transfer was found in ref 55 from plasma electroreflectance data. Taking into acount the direction of charge transfer, we cannot exclude that $P^{Cl}(2\omega)$ contribution compensates (partly or completely) the decrease of $P_{iso}{}^{m}(2\omega)$.

At this stage, we conclude that the effects of Keggin anions and chloride on SHG in the hydrogen region are opposite. The problem of polytungstates inherent contribution to SHG $P^{W}(2\omega)$ will be discussed in more detail in the next subsection.

No pronounced difference of SiW12 and PW12 effects is observed for H−UPD region (Figure 5c, bottom curve in 6b): position and depth of minimum demonstrates no correlation with formal redox potentials and coulometric features (Figure 5c). Minimum potential (point B, Figure 6) is certainly more positive than the formal potential of SiW12 and noticeably more negative than the same value for PW12. Correspondingly, under equilibrium conditions the latter anion should be evidently adsorbed in the reduced state (having different electronic distributions). Similarity of SHG signals wins over the hypothesis of minor $P^{W}(2\omega)$ contribution and supports the interpretation of SHG decrease as induced by the pronounced changes in the state of adsorbed hydrogen.

Double-Layer Region. The behavior of SHG in supporting 0.5 H_2SO_4 solution is much more uncertain. Highly degraded asymmetric SHG maximum, which we observed in background experiments (dashed curve in Figure 5c), is less pronounced than the same feature reported in refs 38, 39, and 42 and resembles a plateau usually observed for polycrystalline Pt in perchloric acid.[38−41] It is easy to see from comparative studies[39] that double-layer SHG response of polycrystalline platinum in sulfuric acid is sensitive to the mode of optical measurements and is not obligatory proportional to sulfate surface coverage. We never observed minimum at 0 V (SCE) (∼0.27 V (RHE) when measuring background curves in 0.5 H_2SO_4 before each series of experiments (this minimum is typical for curves presented in refs 38, 39, and 42).

The general trend of SHG versus potential curves in polytungstate-containing solutions is similar to the trend of "sulfate" curves in refs 38, 39, and 42. It also looks like a curve for isotropic SHG component for Au(111) in sulfate-containing solutions.[56] Actually, the typical shape of these curves corresponds to the growth of anion surface coverage with positive electrode charge and subsequent decrease of coverage resulting from competitive adsorption of oxygen. In the framework of this simplified approach, one can conclude from Figure 6 that surface coverage with PW12 increases significantly with its bulk concentration, and no complete monolayer is formed at sub-mM concentrations (in contrast to polytungstate adsorption on mercury).[8,20] However, not only coverage but also the adsorbate electronic state can be responsible for its effect on SHG signal. To separate two aspects of this problem (changes of $P_{iso}{}^{m}(2\omega)$ and $P^{W}(2\omega)$ contributions), more versatile optical study is required.[57] At this stage, we are limiting ourselves by a qualitative analogy helpful for clarification of this problem.

In contrast to heteropolyacids, isopolytungstates are unstable in acid and less soluble in reduced form. It is possible[27] to prepare long-lived metastable solution of isopolytungstate and to deposit a solid crystalline film in which quasi-reversible W(VI/V) redox transformations take place. Composition of nonstoichiometric film can be presented by a formula of hydrated tungsten bronze $H_xWO_3{*}mH_2O$. Our recent in-situ Raman study[58] provided direct evidence of potential-induced x changes and confirmed previous coulometric estimates:[27] the total change of x at $E > 0$ (RHE) does not exceed 0.1. So, the reduction degree is much lower than for previously reported

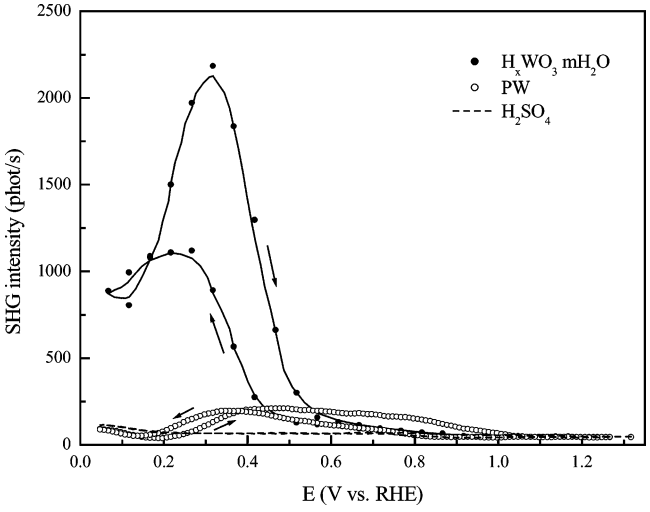

Figure 8. SHG vs potential curves of polytungstate film (ca. 300-nm thick) on Pt in 0.5 M H_2SO_4 (solid symbols). Curves for 0.5 H_2SO_4 + 10 mM PW12 (open symbols) and for background (dashed curve) are given for comparison. Scan rate 10 mV s^{-1}.

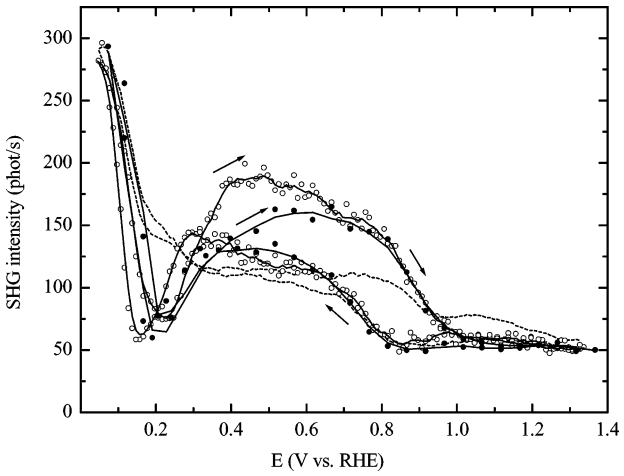

Figure 9. SHG vs potential curves in 0.5 M H_2SO_4 + 0.5 mM PW12. Scan rates are 10 (open symbols) and 50 (solid symbols) mV s^{-1}.

films deposited at ca. −1 V (RHE) from solutions of Keggin anions.[59] (These films[59] resulting from multielectron reduction hardly contain Keggin anions, more probably their destruction products. The latter can be in particular isopolytungstates.)

Figure 8 demonstrates that a so small change of tungsten oxidation degree already results in appearance of very high SHG signal. As the film is ca. 300-nm thick (thickness was estimated according to ref 27), this effect can hardly be referred to interfacial nonlinear response. It is induced by appearance of reduced W(V) which turns the film blue already at very low x.[58] Unfortunately, the film is photosensitive, and its rechargeability decreases under radiation. To check the reasons of low reversibility of SHG curve in Figure 9, one needs more protective irradiation mode. Most probably hysteresis is induced by peculiarities of charge transport inside the film.

In any case, data in Figure 8 confirm that partly reduced tungstate can behave as a dye and can give an essential $P^{W}(2\omega)$ contribution. This gives us a possibility to extend the conclusion[25] about similarity of optical behavior of tungstate-containing solids and molecules in solution and to state the analogy of 3-D film and adsorbed molecules. Another analogy seems to be useful: the shape of SHG-potential curve for polycrystalline platinum modified by adsorbed organic dye[42] looks similar,

having a maximum and demonstrating decrease of signal resulting from dye redox transformation (color change).

Our operational hypothesis named below "molecular UPD" is as follows: inherent SHG contribution of adsorbed Keggin anions $P^W(2\omega)$ results from their partial reduction. For adsorbed species, the reduction is not forbidden even at potentials more positive than equilibrium W(VI/V) potential (by analogy with UPD of monatomic species). It is rather natural to assume that at given potential the reduction degree of adsorbed PW12, with its more positive equilibrium potential, is higher than for SiW12. So, already at this stage our rather qualitative hypothesis explains why SHG signal in the double-layer region is always lower for SiW12 (at fixed concentration, compare two upper curves in Figure 6a).

O−UPD Region. SHG signal decrease at $E > 0.6-0.7$ V (RHE) was observed earlier in refs 38, 39, and 42 for perchloric, sulfuric, and chloride solutions. It was unambiguously attributed to oxygen adsorption. Qualitative reason of this decrease is charge transfer from metal to adsorbate. The decrease is not very strong, and under some optical modes it was not observed for polycrystalline Pt in perchloric acid.[40,41] For Pt single crystals, in combination with anisotropic component, even an opposite sign of oxygen effect was reported.[45]

The oxygen region in our background SHG curves (Figures 5c, 6a, and 7) clearly demonstrates an intermediate step thus discovering various types of oxygen−platinum interactions at lower and higher oxygen coverage. This feature is also slightly distinguishable in some curves presented in refs 38 and 39.

For anodic scans in PW12-containing solutions, SHG signal in O−UPD region is higher than the background signal. Only minor effects are observed for SiW12. The most pronounced qualitative effects manifesting themselves in the difference of anodic and cathodic scans are discussed in the next section.

Hysteresis Phenomena and Possible Mechanisms of Partial Reduction in Adlayer. The accumulation procedure applied in our study cannot guarantee the precise determination of hysteresis for the regions of very sharp signal increase. For a typical scan rate of 10 mV s^{-1}, the existence of hysteresis can be concluded only if the difference of anodic and cathodic scans exceeds 10−20 mV. For less sharp growth/decrease even 20 mV width hystereses are reliable.

Our observations of hysteresis in the region of high hydrogen coverages are on the verge of this accuracy limit. SHG loops in H−UPD region can be also found in refs 38−40 for scan rates of 5−10 mV s^{-1}, but there is no histeresis in ref 42 at 50 mV s^{-1}. We believe that all these effects come from registration problems and give no evidence of any irreversibility of hydrogen adsorption−desorption.

An opposite statement should be evidently referred to hysteresis in the O−UPD region. It is much wider and belongs to the region of slow signal changes with potential, so signal accumulation details cannot induce any false hysteresis. Position of "oxygen SHG loop" in 0.5 M H_2SO_4 and chloride-containing solutions (Figure 6) demonstrate excellent agreement with voltammetric O−UPD features.

Reliability of hystereses of SHG curves in the double-layer region is also undoubtful for polytungstate-containing solutions and is even more pronounced as compared to the oxygen loop. Double-layer hysteresis increases with PW12 concentration (Figure 6a). Hysteresis of ascending branch of the curves (at the boundary of hydrogen adsorption region) is less pronounced than in the double-layer region. It becomes reliable only for high (>1 mM) bulk polytungstate concentrations. All these features (but less pronounced) are also observed for SW12.

If we apply a 5 times higher scan rate (Figure 9), the cathodic scan remains practically unchanged, when the decrease of SHG signal is observed for anodic scan. At the same time, the accessible decrease of the scan rate does not affect the shape of the loop, demonstrating that a slow process responsible for hysteresis at 10 mV s^{-1} has a much slower time scale. For 10 mV s^{-1}, we observe a steady-state behavior determined by the process with relatively fast equilibration, when the most slow process remains "frozen". This situation is similar to oxygen adsorption,[60] when various forms of oxygen adatoms differ strongly in adsorption kinetics, and at certain time scales only some of them can be observed.

A difference in the peculiarities of slow tungstate adlayer equilibration for two opposite scan directions (Figure 9) can be associated with the difference in initial orientations, slow self-assembling phenomena, charge-dependent number of oxygen atoms forming bonds with Pt, and so forth. All these versions look realistic taking into account molecular level data for Ag electrodes.[10−12,14,15] A feature specific for Pt is an accelerated equilibration at the boundary of H−UPD region, which manifests participation of hydrogen adatoms in this process. In addition to our general operating hypothesis, one of the possible mechanisms of molecular UPD can be chemical partial reduction of adsorbed anions by hydrogen adatoms. If being so, much more slow partial reduction at cathodic scan can be explained by the absence of hydrogen adatoms in the adlayer. (Characteristic times of this slow equilibration seem to be outside of mV/s time scale usually used in CV studies. Potentiostatic tests are in progress to clarify this problem.) Immediately, when these species appear (at ca. 0.35 V (RHE)), time limitations of adlayer equilibration become less pronounced. This extended hypothesis gives explanation of excess charge (Figure 4) which appears just at the right boundary of H−UPD region. The phenomenon can be also considered as a sort of hydrogen spillover because if a portion of hydrogen atoms is spent for tungstate reduction, new hydrogen atoms appear at vacant positions. Corresponding estimates are presented in the conclusive section.

SHG hysteresis in the H−UPD region which appears at higher bulk concentrations of PW12 indicates the shortage of H adatoms necessary for equilibration. This is possible only if polytungstate coverage really increases with concentration. Disturbance of hydrogen adlayer (SHG decrease in point B, Figure 6) also increases with concentration, but only for anodic scans (solid points in the bottom curve, Figure 6b).

Shorter scans (with cathodic potential limit of 0.29 V(RHE)) repeat exactly corresponding sections of curves presented above. We interpret this fact as the confirmation of potential-dependent polytungstate coverage. Actually, if a lot of polyanions are already adsorbed at $E < 0.29$ V (RHE), they never feel shortage of H adatoms at more positive potentials.

An important feature is also observed for the right-hand edge of the O−UPD region. Oxygen hysteresis is completely suppressed in PW12-containing solutions (and noticebly decreases in the presence of SiW12) at $E > 1$ V(RHE). Both anodic and cathodic scans in this region coincide with a cathodic scan of background curves. This means that in the presence of polytungstates the state of adsorbed oxygen is more close to its quasi steady state at higher coverage. In this connection, a minor influence of polytungstates on voltammetric peak of oxygen desorption is not surprising.

Self-Consistency of Molecular UPD Hypothesis. To estimate the conformity of our assumptions with CV data, we apply the following adlayer model which exploits ball-like geometry and large size of Keggin anions. For such type of species, even

TABLE 1: Characteristic Potential Regions and Corresponding Events in Adlayer

potential region (scan direction)		polytungstate coverage vs E	partial W(VI/V) reduction in adlayer	tungstate location	schematic illustration, Figure 10
H−UPD	<0.25 V	very low	rather high	surrounded by H_{ad}	a
	>0.25 V	increases		mixed with H_{ad}	b
double layer, <0.65 V	anodic cathodic	continues to increase	starts to decrease	directly at Pt surface	c
double layer, > 0.65 V	anodic cathodic	nonequilibrium	inhibited	separated by oxygen	d
O−UPD <1 V	anodic	probably starts to decrease	already absent	surrounded by O_{ad}	e
O−UPD >1 V	cathodic	nonequilibrium still nonzero		separated by oxygen	f

close-packed adlayers are rather loose, as the areas between the neighboring adsorbed species are wide enough, giving a chance for low-molecular adsorbates to contact the surface. This assumption agrees with STM data for SiW12 anion on Ag (see ref 14, for example). An additional possibility of coadsorption appears if the species which penetrated into the areas between adsorbed polytungstate anions are able to move along the surface to occupy positions under "balls". Actually, each Keggin anion occupies 15−16 surface atoms, but only 1−4 of them take part in the adsorption interaction. The others are shaded by adsorbate projection but are available for smaller foreign adsorbates. This can be judged from the number of external oxygen atoms, which find themselves at the closest distance to the surface. Correspondingly, only 5−20% of Pt atoms can be completely blocked by polytungstate, when all others are simply more or less screened. Moreover, about 25% of the surface consists of the areas between anion projections. No complications are expected for adsorption of foreign species at these areas.

If we assume that the molecular UPD region is located at potentials more positive than equilibrium potential for one-electron anion reduction, we should allow for transfer of one electron per each W12 unity which occupies 15−16 surface atoms. Taking into account geometry and coverage, the upper limit of UPD charge cannot exceed 6−7% of usual H−UPD charge (which corresponds, under the first approximation, to one electron per one surface atom). This effect is comparable (slightly lower) than experimental excess charge, but self-consistency requires simultaneous assumption of unchanged quantity of coadsorbed hydrogen. As the first and the second W(VI/V) reduction potentials are very close, a higher degree of reduction can be also assumed, which provides quantitative agreement. Sulfate displacement by tungstates can change hydrogen adatom sublattice and can result in a slight increase of hydrogen adatom coverage. This assumption explains the changes of adsorbed hydrogen state in the closest vicinity of zero RHE potential (bottom curve in Figure 6b).

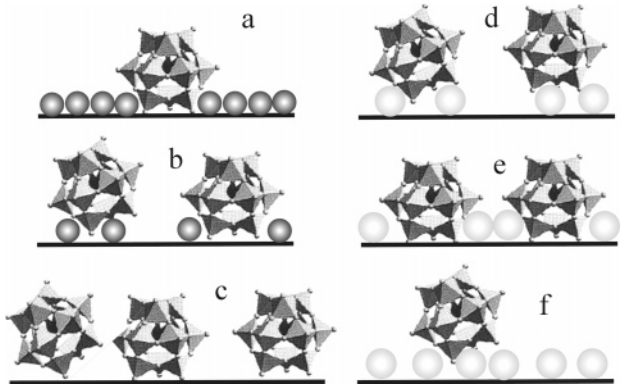

Figure 10. Schematic configurations of adlayers corresponding to various potential regions and scan directions (see Table 1).

The same geometric interpretation looks reasonable also for polytungstate effects on O−UPD. Suppression of the latter process (as seen from CV data) agrees with the assumption of selective blocking of only 5−10% of surface atoms, and this value agrees with a model of tungstate attached to the surface via its one or two external oxygen atoms. Starting from c.a. 1−1.1 V (Figure 5b), this O−UPD suppression turns to noticeable additional oxygen adsorption, and simultaneously oxygen hysteresis disappears from SHG curves. The most simple explanation is oxygen penetration between polytungstates and metal (without complete desorption of the former). If being so, these "under-tungstate" positions should correspond to more strong oxygen bonding, giving rise to an additional decrease of SHG at $E > 1$ V (Figures 5c, 6a, 9). It is easy to notice that at $E = 0.65-0.95$ V (RHE) there is no difference of cathodic SHG scans for supporting and polytungstate-containing solutions. This is expected if oxygen adatoms remain between the surface and polyanion up to complete desorption. Now, we can enclose all phenomena under discussion and state that one of the possible reasons for slow equilibration of adlayer when scanning potential from anodic side is separation of anions and metal surface which inhibits direct partial charge transfer.

Conclusions

SHG data provide exact evidence of Keggin anions adsorption on Pt in the overall potential range, including hydrogen and oxygen adsorption regions. The proposed description of events taking place in adlayer at various potentials is summarized in Table 1 and in Figure 10. Manifestations of mutual interactions of coadsorbed species are found and explained in the framework of molecular UPD hypothesis.

Acknowledgment. This work is supported by the Russian Foundation for Basic Researches (RFBR, project 03-03-39012), the Council for Grants of President of Russian Federation for leading scientific schools (NSh-2089.2003.3), Research for the Future (RFTF) Program, and the Japanese Society for the Promotion of Science.

References and Notes

(1) Klemperer, W. G.; Wall, C. G. *Chem. Rev.* **1998**, *98*, 297.
(2) Coronado, E.; Gomez-Garcia, C. J. *Chem. Rev.* **1998**, *98*, 273.
(3) Muller, A.; Peters, F.; Pope, M. T.; Gatteschi, D. *Chem. Rev.* **1998**, *98*, 239.
(4) Kozhevnikov, V. I. *Chem. Rev.* **1998**, *98*, 171.
(5) Mizuno, N.; Misono, M. *Chem. Rev.* **1998**, *98*, 199.
(6) Sadakane, M.; Steckhan, E. *Chem. Rev.* **1998**, *98*, 219.
(7) Yamase, T. *Chem. Rev.* **1998**, *98*, 307.
(8) Rong C.; Anson F. C. *Anal. Chem.* **1994**, *66*, 3124.
(9) Rong, C.; Anson, F. C. *Inorg. Chim. Acta* **1996**, *242*, 11.
(10) Ge, M.; Zhong, B.; Klemperer, W. G.; Gewirth, A. A. *J. Am. Chem. Soc.* **1996**, *118*, 5812.
(11) Kim, J.; Gewirth, A. A. *Langmuir* **2003**, *19*, 8934.

(12) Teague, C. M.; Li, X.; Biggin, M. E.; Lee, L.; Kim, J.; Gewirth, A. A. *J. Phys. Chem. B* **2004**, *108*, 1974.
(13) Clinton, D. E.; Tryk, D. A.; Bae I. T.; Urbach, F. L.; Antonio M. R.; Scherson, A. D. A. *J. Phys. Chem.* **1996**, *100*, 18511.
(14) Lee, L.; Wang, J. X.; Adzic, R. R.; Robinson, I. K.; Gewirth, A. A. *J. Am. Chem. Soc.* **2001**, *123*, 8838.
(15) Lee, L.; Gewirth, A. A. *J. Electroanal. Chem.* **2002**, *522*, 11.
(16) Keita, B.; Nadjo, L.; Belanger, D.; Wilde, C. P.; Hilaire, M. *J. Electroanal. Chem.* **1995**, *384*, 155.
(17) Tang, Z.; Liu, S.; Wang, E.; Dong, S. *Langmuir* **2000**, *16*, 4946.
(18) Kaba, M. S.; Song, I. K.; Barteau, M. A. *J. Phys. Chem. B* **1996**, *100*, 19577.
(19) Song, I. K.; Barteau, M. A. *Langmuir* **2004**, *20*, 1850.
(20) Borzenko, M. I.; Tsirlina, G. A.; Petrii, O. A. *Russ. J. Electrochem.* **2000**, *36*, 452.
(21) Borzenko, M. I.; Tsirlina, G. A.; Petrii, O. A. *Mendeleev Commun.* **2002**, *12*, 126.
(22) Tze, Wei; Borzenko, M. I.; Tsirlina, G. A.; Petrii, O. A. *Russ. J. Electrochem.* **2002**, *38*, 1250.
(23) Borzenko, M. I.; Chojak, M.; Kulesza, P. J.; Tsirlina, G. A.; Petrii, O. A. *Electrochim. Acta* **2003**, *48*, 3797.
(24) Rocchiccioli-Deltcheff, C.; Fournier, M.; Franck, R. *Inorg. Chem.* **1983**, *22*, 207.
(25) Hiskia, A.; Mylonas, A.; Papaconstantinou, E. *Chem. Soc. Rev.* **2001**, *30*, 62.
(26) Himeno, S.; Takamoto, M.; Ueda, T. *J. Electroanal. Chem.* **1999**, *465*, 129.
(27) Timofeeva, E. V.; Tsirlina, G. A.; Petrii, O. A. *Russ. J. Elecrochem.* **2003**, *39*, 716.
(28) Cai, Lei; Xiao, Xudong; Loy, M. M. T. *J. Chem. Phys.* **2001**, *115*, 9490.
(29) Bonn, M.; Denzler, D. N.; Funk, S.; Wolf, M.; Wellershoff, S.-S.; Hohlfeld, J. *Phys. Rev. B* **2000**, *61*, 1101.
(30) Hohlfeld, J.; Wellershoff, S.-S.; Gudde, J.; Conrad, U.; Jahnke, V.; Matthias, E. *Chem. Phys.* **2000**, *251*, 237.
(31) Kao, F.-J.; Bush, D. J.; Gomes da Costa, D.; Ho, W. *Phys. Rev. Lett.* **1993**, *70*, 4098.
(32) Pope, M. T.; Varga, G. M. *Inorg. Chem.* **1966**, *5*, 1249.
(33) Hevre, G. *Ann. Chim.* **1971**, *6*, 219.
(34) Keita, B.; Nadjo, L. *J. Electroanal. Chem.* **1985**, *191*, 441.
(35) Keita, B.; Nadjo, L. *J. Electroanal. Chem.* **1987**, *227*, 77.
(36) Frumkin, A. N.; Petrii, O. A. *Electrochim. Acta* **1975**, *20*, 347.
(37) Frumkin, A. N.; Petrii, O. A. *Topics in Pure and Applied Electrochemistry*; SAEST: Karaikudi, India, 1975.
(38) Campbell, D. J.; Corn, R. M. *J. Phys. Chem.* **1988**, *92*, 5796.
(39) Campbell, D. J.; Lynch, M. L.; Corn, R. M. *Langmuir* **1990**, *6*, 1656.
(40) Yagi, I.; Nakabayashi, S.; Uosaki, K. *J. Phys. Chem. B* **1997**, *101*, 7414.
(41) Bae, I. T. *J. Phys. Chem.* **1996**, *100*, 14081.
(42) Campbell, D. J.; Higgins, D. A.; Corn, R. M. *J. Phys. Chem.* **1990**, *94*, 3681.
(43) Corn, R. M.; Higgins, D. A. *Chem. Rev.* **1994**, *94*, 107.
(44) Pozniak, B.; Mo, Y.; Stefan, I. C.; Mantey, K.; Hartmann, M.; Scherson, D. A. *J. Phys. Chem. B* **2001**, *105*, 7874.
(45) Lynch, M. L.; Barner, B. J.; Corn, R. M. *J. Electroanal. Chem.* **1991**, *300*, 447.
(46) Lynch, M. L.; Corn, R. M. *J. Phys. Chem.* **1990**, *94*, 4382.
(47) Dzhavakhidze, P. G.; Kornyshev, A. A.; Liebsch, A.; Urbakh, M. *Phys. Rev. B* **1992**, *45*, 9339.
(48) Grubb, S. G.; DeSantolo, A. M.; Hall, R. B. *J. Phys. Chem.* **1988**, *92*, 1419.
(49) Petrii, O. A.; Frumkin, A. N.; Kotlov, Y. G. *Elektrokhimiya* **1969**, *5*, 735.
(50) Frumkin, A. N.; Damaskin, B. B.; Petrii, O. A. *J. Electroanal. Chem.* **1974**, *53*, 57.
(51) Frumkin, A. N.; Damaskin, B. B.; Petrii, O. A. *Z. Phys. Chem.* **1975**, *256*, 728.
(52) Petrii, O. A.; Frumkin, A. N.; Kolotyrkina-Safonova, T. Y. *Elektrokhimiya* **1974**, *10*, 1741.
(53) Petrii, O. A.; Frumkin, A. N.; Kolotyrkina-Safonova, T. Y. *Dokl. Akad. Nauk SSSR* **1975**, *222*, 347.
(54) Petrii, O. A.; Ushmaev, A. V.; Safonova, T. Y. *Elektrokhimiya* **1977**, *13*, 745.
(55) Kazarinov, V. E.; Foontikov, A. M.; Tsirlina, G. A. *J. Electroanal. Chem.* **1990**, *282*, 253.
(56) Mirwald, S.; Pettinger, B.; Lipkowski, J. *Surf. Sci.* **1995**, *335*, 264.
(57) Lipkowski, J.; Shi, Z.; Chen, A.; Pettinger, B.; Bilger, C. *Electrochim. Acta* **1998**, *43*, 2875.
(58) Palys, B.; Borzenko, M.; Tsirlina, G. A.; Jackowska, K.; Petrii, O. A. *Electrochim. Acta* **2004**, *49*, in press.
(59) Keita, B.; Nadjo, L. *J. Electroanal. Chem.* **1987**, *230*, 85.
(60) Angerstein-Kozlowska, H.; Conway, B. E.; Sharp, W. B. A. *J. Electroanal. Chem.* **1973**, *43*, 9.